Do peatland microforms move through time? Examining the developmental history of a patterned peatland using ground-penetrating radar

Nicholas Kettridge,[1] Andrew Binley,[2] Xavier Comas,[3] Nigel J. Cassidy,[4] Andy J. Baird,[5] Angela Harris,[6] Jan van der Kruk,[7] Maria Strack,[8] Alice M. Milner,[9] and James M. Waddington[10]

Received 30 September 2011; revised 12 July 2012; accepted 21 July 2012; published 18 September 2012.

[1] Using ground-penetrating radar (GPR) to map subsurface patterns in peat physical properties, we investigated the developmental history of meso-scale surface patterning of microforms within a raised bog. Common offset GPR measurements were obtained along a 45-m transect, at frequencies ranging from 100 to 900 MHz. We found that low-frequency (central frequency < 240 MHz) GPR could not adequately represent the subsurface structures of the peatland because individual peat layers were too thin. However, more detailed high-frequency measurements (central frequency ≥ 240 MHz) showed a striking pattern of subsurface reflections that dip consistently in a northerly direction. The angle of these dipping reflectors is calculated using a semblance algorithm and was shown to average 3.9° between a depth of 1.0 and 2.5 m. These dipping reflectors may indicate downslope migration of surface microforms during the development of the peatland. Based on the estimated angle and the rate of peat accumulation, the average rate of downslope propagation of these surface microforms is calculated at 9.8 mm per year. Further survey work is required to establish whether the downslope migration is common across the peatland.

Citation: Kettridge, N., A. Binley, X. Comas, N. J. Cassidy, A. J. Baird, A. Harris, J. van der Kruk, M. Strack, A. M. Milner, and J. M. Waddington (2012), Do peatland microforms move through time? Examining the developmental history of a patterned peatland using ground-penetrating radar, *J. Geophys. Res.*, *117*, G03030, doi:10.1029/2011JG001876.

1. Introduction and Aim of Research

[2] Northern peatlands represent an important global carbon store (containing ~220–460 Pg C [*Gorham*, 1991; *Turunen et al.*, 2002]). The thermal, hydrological, ecological and biogeochemical functioning of these environments varies strongly at the fine spatial scales (10^0–10^1 m) associated with the surface micro-topography of hummocks, hollows, lawns and pools [*Kettridge and Baird*, 2010; *Whittington and Price*, 2006; *Waddington and Roulet*, 1996]. Any alterations to the proportion or spatial arrangement of these microforms will likely have an important effect on the eco-hydrological and biogeochemical form and function of these ecosystems [*Baird et al.*, 2009], potentially producing strong nonlinear responses in the carbon balance [*Belyea*, 2009; *Bubier et al.*, 1993].

[3] Peatland microforms show strong self organization, producing recognizable patterns [*Foster and Fritz*, 1987; *Boatman and Tomlinson*, 1973; *Tallis*, 1994]. While the current spatial organization of such microforms is easily observable across the peatland surface, additional detailed information regarding their past organization and development is recorded within the peatland stratigraphy. Different microforms lay down peat with different physical properties during the development of the peatland, providing evidence of past transitions between different microforms and their movement or expansion over time. By mapping this rich archive we can determine the developmental pathways of the peatland microforms and, in combination with the expanding suite of mathematical models which have the potential to

[1]School of Geography, Earth and Environmental Sciences, University of Birmingham, Edgbaston, Birmingham, UK.
[2]Lancaster Environment Centre, Lancaster University, Lancaster, Lancashire, UK.
[3]Department of Geosciences, Florida Atlantic University, Davie, Florida, USA.
[4]School of Physical and Geographical Sciences, Keele University, Keele, Staffordshire, UK.
[5]School of Geography, University of Leeds, Leeds, UK.
[6]Geography, School of Environment and Development, University of Manchester, Manchester, UK.
[7]Institute of Bio- and Geosciences, Forschungszentrum GmbH, Jülich, Germany.
[8]Department of Geography, University of Calgary, Calgary, Alberta, Canada.
[9]Department of Geography, University College London, London, UK.
[10]School of Geography and Earth Sciences, McMaster University, Hamilton, Ontario, Canada.

Corresponding author: N. Kettridge, School of Geography, Earth and Environmental Sciences, University of Birmingham, Edgbaston, Birmingham B15 2TT, UK. (n.kettridge@bham.ac.uk)

0148-0227/12/2011JG001876

simulate the organization of hummocks and hollows over time [cf. *Morris et al.*, 2011, *Baird et al.*, 2012; *Eppinga et al.*, 2009], identify the key ecohydrological controls on pattern development.

[4] Peatland stratigraphy may be inferred from multiple peat cores [*Barber et al.*, 1998]. Distinct changes in the physical properties of the peat across the peatland, evident within multiple peat cores, suggest a peatland-wide shift in its ecohydrological functioning [*Belyea*, 2009; *Belyea and Malmer*, 2004]. However, alterations to the proportion, arrangement or spatial organization of peatland microforms are more difficult to ascertain from coring. A dense distribution of peat cores at the decimeter scale would be required because of the fine scale of patterning across many peatlands (often less than 1 m [*Foster and Fritz*, 1987]), and the need to identify contiguous peat layers (through dating or pollen analysis) across multiple cores. This intensity of coring is time consuming, destructive, and prevents the spatial distribution of peat physical properties being obtained at the hillslope scale (10^2 m). Alternatively, exposed peat faces could be surveyed. However, this type of analysis is not practical for intact peatlands or those mined by modern harvesting techniques. In addition, it is not always clear how surface patterns and peat layers were altered by the associated drainage operations or how much of the upper peat profile was lost to mining or degradation. In comparison, ground-penetrating radar (GPR) has the potential to map boundaries between different peat layers in undisturbed peatlands at high (sub-microform) resolution at the hillslope scale [*Worsfold et al.*, 1986].

[5] GPR is a non invasive geophysical technique used to identify changes in the dielectric permittivity of a medium. A high frequency electromagnetic (EM) wave, generated from a transmitting antenna, penetrates the subsurface and is reflected from boundaries between layers of contrasting electric properties. These reflections are recorded by a second, receiving, antenna. In common offset surveys, the antennas are kept at a constant separation and measurements are obtained along the length of a transect by moving the antennas in unison. Common offset measurements have been used to characterize peat thickness for over 30 years [e.g., *Ulriksen*, 1980; *Warner et al.*, 1990, *Theimer et al.*, 1994; *Slater and Reeve*, 2002], identifying the boundary between the peat and the mineral interface. Nevertheless, linking individual reflections to specific boundaries within the peat profile has proved problematic [e.g., *Worsfold et al.*, 1986]. Only boundaries between very distinct, spatially extensive, layers have been matched clearly to GPR reflections, either between very poorly decomposed peat and well-decomposed peat [*Warner et al.*, 1990] or between layers of high and low wood content [*Comas and Slater*, 2009]. However, geophysical investigations have often focused at the peatland scale, where lower vertical (low-frequency) and horizontal (large step size) resolution measurements have been used to visualize the peat-mineral interface [*Comas et al.*, 2004; *Jol and Smith*, 1995]. In comparison, detailed visual analysis of peat properties on short peat faces (c. 4 m in length) has highlighted the complex spatial distribution of boundaries between different types of peat over scales of decimeters [*Barber*, 1981; *Walker and Walker*; 1961] and thus the need for high frequency geophysical measurements at a high spatial resolution.

[6] The aim of the research reported herein, was to examine the developmental history of a series of microforms on one peatland using high-resolution GPR measurements. In so doing, we aimed to provide a balanced assessment of GPR as a non-invasive means to discern stratigraphic detail within intact peat deposits, with specific emphasis on identifying the measurement resolutions that provide the most detailed and most representative characterization of the subsurface peat boundaries. This will identify whether the GPR technique can provide useful future data from which to test peatland development models.

2. Study Design and Methods

2.1. Study Site

[7] Measurements were performed at Cors Fochno (52°31′N, 4°1′W), a lowland raised bog in west Wales (Figure 1a; see *Baird et al.* [2008] for an additional map showing the topography of the surrounding area). Away from the central portion of the peatland, drainage ditches have been constructed and areas to the southwest and southeast have been hand cut to approximately two spade depths (c. 60 cm). However, the more central portion of the peatland, within which this study was conducted, has been unaffected by such mining activities. Within this central dome where the peat is over 6.5 m deep, hummock, lawn and hollow microforms are clearly identifiable. Hummocks are dominated by ericaceous shrubs such as *Calluna vulgaris* (L.) Hull. and Sphagna such as *Sphagnum capillifolium* (Ehrh.) Hedw. and *Sphagnum fuscum* (Schimp.) Klinggr. Lawns are covered with Sphagna such as *Sphagnum magellanicum* Brid. and sedges such as *Eriophorum angustifolium* Honck. Hollows are dominated by *Sphagnum pulchrum* (Lindb. ex Braithw.) Warnst. and vascular plants including *Rhynchospora alba* (L.) Vahl. and *Menyanthes trifoliata* L. [*Baird et al.*, 2008]. The hummocks and hollows are arranged in a fine scale maze-like pattern (Figure 1b), with inter-connected regions of drier peat (hummocks/ridges), distributed across a wetter peatland composed of hollows and lawns.

[8] Measurements were conducted along a 45-m transect that crossed a series of sub-parallel linear hummocks, lawns and hollows (Figure 1b). The context of the transect within the peatland dome as a whole can be seen in Figure 1c, which represents an interpolation of 2-m resolution Lidar data along a N-S axis on which the transect lies. From Figure 1c it can be seen that the transect sits within the central portion of the peatland, to the southern side of the highest part of the dome.

2.2. Ground-Penetrating Radar Surveys

[9] Common offset measurements were taken along the length of the 45-m transect at 100, 200, 225 and 450 MHz. Common offset measurements were also taken on a short 6-m section of the transect at a frequency of 900 MHz. Unshielded 100 and 200 MHz measurements were collected using a Sensors and Software pulse EKKO 100 unit, with a step size of 0.10 m and an antenna separation distance of 1.0 and 0.5 m, respectively. Shielded 225, 450 and 900 MHz measurements were performed at a step size of 0.05, 0.025 and 0.02 m, respectively, at an antenna separation of 0.5, 0.25 and 0.17 m. Each trace was stacked 16 times to increase the signal-to-noise ratio. Processing of the common offset measurements

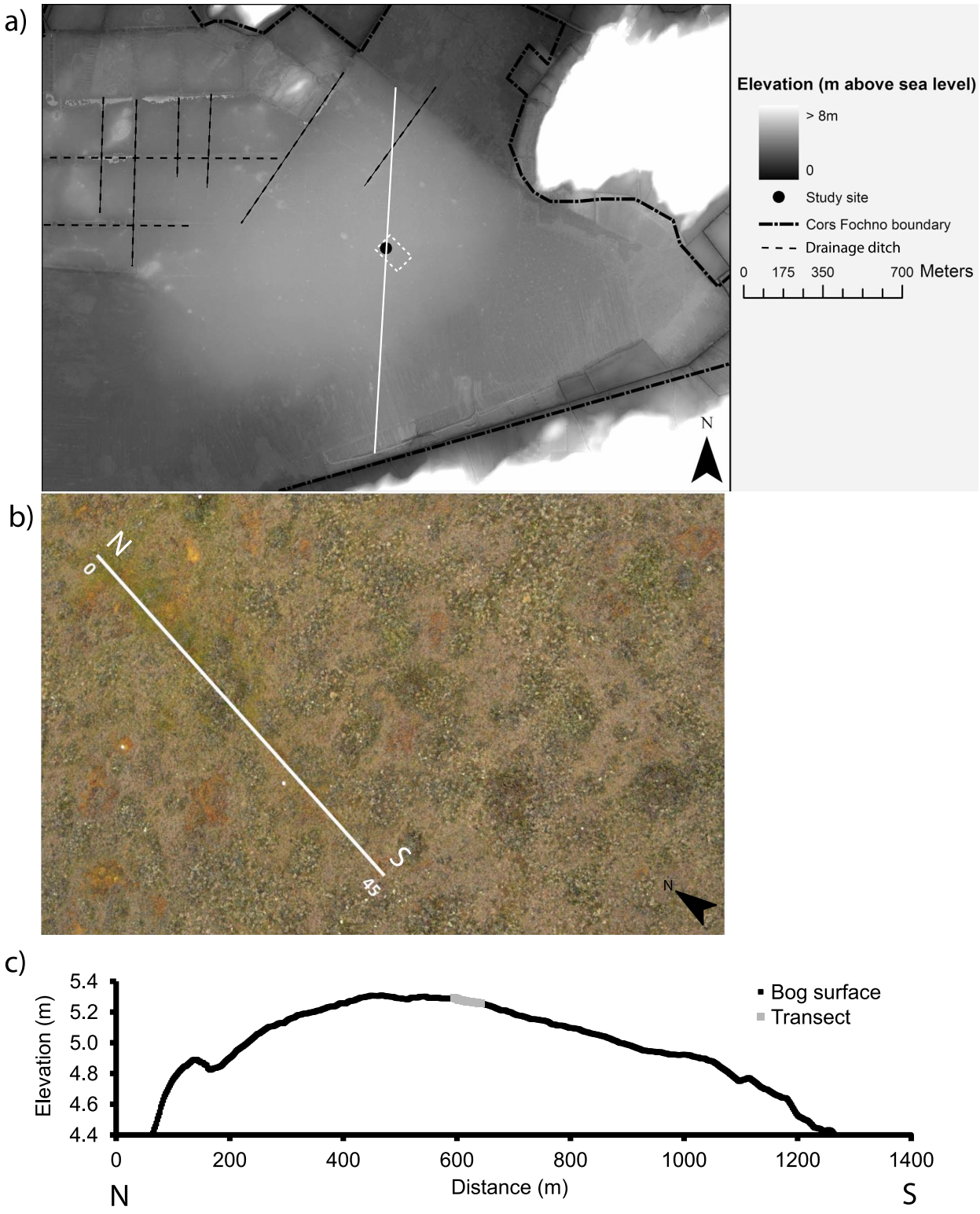

Figure 1. (a) Digital elevation model of the studied peatland and surrounding region. (b) Aerial photograph of the zone defined by the white dotted box within Figure 1a, which includes the 45-m transect and the surrounding area of peatland. Photo taken approximately two years after the GPR surveys using a kite-borne camera. The location of the 45-m transect is marked by the white line with the associated distances in meters. (c) Elevation of the peat surface along the extended transect (represented by the solid black line) derived from LIDAR measurements. The location of the 45-m transect is marked in gray; elevation varies by 3.5 cm over the length of this transect.

consisted of: a) a "dewow" filter to correct for low-frequency noise; b) a time-varying gain to equalize amplitude variation associated with attenuation of the EM signal with depth; c) a bandpass filter to eliminate high- and low-frequency noise; d) a static correction to eliminate the time delay between trigger and recording; e) a topographic correction to correct for topography; and f) a fk migration (Stolt) in order to correct distortions and dip displacements due to the 3D nature of EM wave radiation [cf. *Neal*, 2004]. The depth of reflections within the common offset profile were calculated assuming an average EM velocity of 0.036 m ns^{-1}, calculated at the study site from common mid-point surveys collected along the transect (cf. X. Comas et al., in preparation).

[10] To determine an objective measure of the pattern of reflections, we employed a geometric attributes program based on the work of *McClymont et al.* [2008], written by J. Doetsch (ETH, Zurich, Switzerland). The apparent dip angles of the reflections were calculated based on the semblance algorithm of *Marfurt et al.* [1998]. At discrete intervals along each trace, semblance (continuity in the EM signal) is calculated for hypothetical directions away from the point, with ranges of apparent dip varying between −40° and +40° across adjacent traces. The apparent dip is equal to the hypothetical direction with the highest semblance [for further details, see *McClymont et al.*, 2008].

2.3. Von Post Peat Humification Survey

[11] Peat properties through the top 6.5 m of the profile were analyzed at three locations, at a distance of 12, 28 and 37.5 m along the transect—within a hollow, at the boundary between a hummock and hollow, and within a hummock, respectively. Cores of peat were extracted in 0.5-m long sections using a Russian corer, 45 mm in diameter. Boundaries between layers of peat were identified by visual inspection in the field. Boundaries were identified according to visible differences between peat layers even if the estimate of humification only placed the peat either side of the boundary one von Post unit (see below) apart. Each layer of peat was analyzed in the field to interpret its structure (firm, plastic, loose, watery), the abundance of the plant functional types (sedges, *Sphagnum* mosses, woody shrubs), and the genus or species where identifiable. The ratio of sedge to *Sphagnum* was calculated from the comparative abundance of sedge to *Sphagnum* (3 = greater abundance of sedge, 2 = approximately equal abundance of sedge and *Sphagnum*, 1 = greater abundance of *Sphagnum*). The peat within each core was also classified using the von Post scale [*von Post and Granlund*, 1926], which denotes the degree of humification of the peat, and ranges from a value of H-1, denoting unhumified peat or fresh litter, through to H-10, that represents completely humified (amorphous) peat with no discernible plant remains [*Ekono, Inc.*, 1981]. For some core sections, the observers tested their interpretations by independently noting boundaries between layers and by independently classifying the properties of each layer. These tests showed that the observers were always within a von Post score of each other and that they almost always agreed on the firmness and textural classification. Therefore, we can be confident that the classification, even when carried out by different (single) observers, was comparable between core locations.

[12] An additional, spatially intensive, survey of peat properties through the top 2 m of the profile was performed over a short 2.1-m long section of the transect, starting within a hollow and ending in an adjacent hummock. Peat cores through the top 2 m of the peat profile were extracted with a second 1.0-m Russian corer, 45 mm in diameter, at 0.3-m intervals along the transect. Peat cores within the spatially intensive survey were extracted relative to a fixed horizontal datum. The datum consisted of a horizontal metal pipe that nestled in sockets on two plastic pipes driven vertically into peat to a depth of 0.9 m. The metal pipe was held in place via cable ties. A spirit level was used initially to level the datum and to confirm that the datum stayed level during two days of coring. All core depths, and peat boundary depths, were measured relative to this datum, to an accuracy of better than +/−0.01 m, and then corrected to the peat surface at the first core. Peat cores were analyzed using the protocol for the 6.5-m peat cores described above.

3. Results

3.1. Von Post Survey

[13] Along the full length of the transect, the level of peat decomposition increased rapidly with depth through the top 0.5 m of the profile (Figure 2a). Within two of the three 6.5-m peat cores, the von Post score increased from H-1 to H-10 within this short distance. In the third core, at a distance of 37.5 m along the transect within a hummock microform, the von Post score increased to H-10 from an initial H-7 within the top 0.65 m. After this initial increase, the peat remained well decomposed through the depth of the profile, with only small variations in level of decomposition; principally in the top 2 m and from a depth of 5–6 m (Figure 2a). While the von Post score varied little below a depth of 0.5 m, clear transitions in peat type, composition and structure occurred with depth. Through each of the profiles, the structure of the peat fluctuated between plastic, loose and watery (Figure 2b), and the composition of the peat varied in the ratio of *Sphagnum* to sedge remains (Figure 2c).

[14] The spatially intensive coring results highlighted the complex fine-scale variation in the peat boundaries over distances of less than 2 m (Figure 3a). However, within this complex 2-D structure, key boundaries were identifiable. At a depth of 0.3 m a horizontal boundary ran across all eight cores between peat of H-3–H-4 and H-4–H-5. At a depth of 0.6–0.8 m, a boundary was evident across which the peat decomposition decreased with depth from H-7 to H-3, and at a depth of 0.9 m there was a transition to more decomposed peat of H-8 to H-9. In addition, at a depth of 1.0 m, a sharp horizontal transition from H-7–H-8 to H-3–H-5 was evident. This transition occurred at the boundary between the two 1-m sections of each 2.0-m core and, as a result, may have been artificially 'sharpened'. The zone of more poorly decomposed peat beneath this boundary extended to a depth of 1.7 m before a transition to more decomposed peat of H-8 to H-9.

3.2. Common Offset Measurements

[15] Figure 3c shows a GPR common offset obtained along a portion of the 45-m transect and over the length of the high-resolution core data using 225 MHz antennas. Each individual trace represents a vertical display of amplitudes along the waveform as it travels through the subsurface and encounters changes in the relative dielectric permittivity. Positive amplitudes are indicated in black while negative

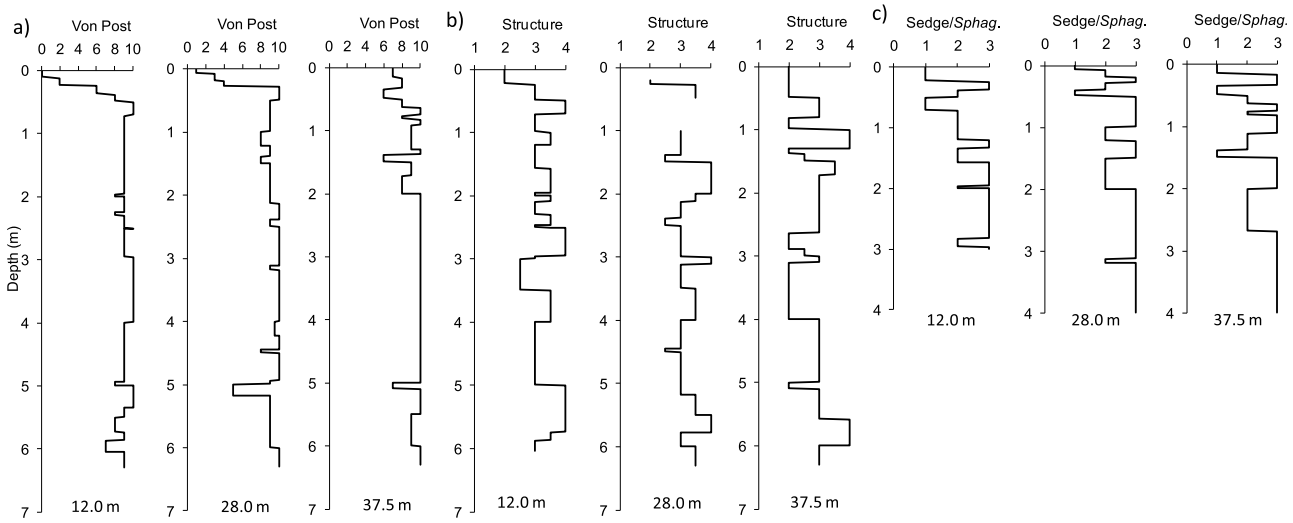

Figure 2. (a) Von Post score, (b) peat structure and (c) ratio of sedge to *Sphagnum* in cores along the 45-m transect. Vertical variations in each property are represented at three locations within three separate graphs. Each graph represents individual cores at a distance of 12.0, 28.0 and 37.5 m alone the transect (indicated at the bottom of each plot). Peat structure is defined on an ordinal scale, 1-firm, 2-plastic, 3-loose or 4-watery. Ratio of sedge to *Sphagnum* presented as, 1-greater proportion of *Sphagnum* than sedge, 2-equal proportions of *Sphagnum* and sedge, 3-greater proportion of sedge than *Sphagnum.* The abundance of plant functional types is presented to a depth of approximately 4 m (at greater depths abundance could not be identified visually).

values are shown in white. The EM wave initially moves from transmission in the air to transmission into the ground resulting in a complex reflection pattern, or ground coupling [*Reynolds*, 1994]. This produces a strong stratigraphical boundary in the near surface where none exists (Figure 3d). Individual reflections follow below and also consist of several wavelets indicative of changes in physical properties of the subsurface. A complete review of radar attributes in GPR profiles for stratigraphic applications is given by *Neal* [2004]. Common offset measurements for the entire transect using 100 MHz, 225 MHz and 450 MHz antennas are presented in Figure 4 with the associated classification of the surface microforms along the transect (Figure 4a). The 100-MHz measurements showed a clear pattern of horizontal,

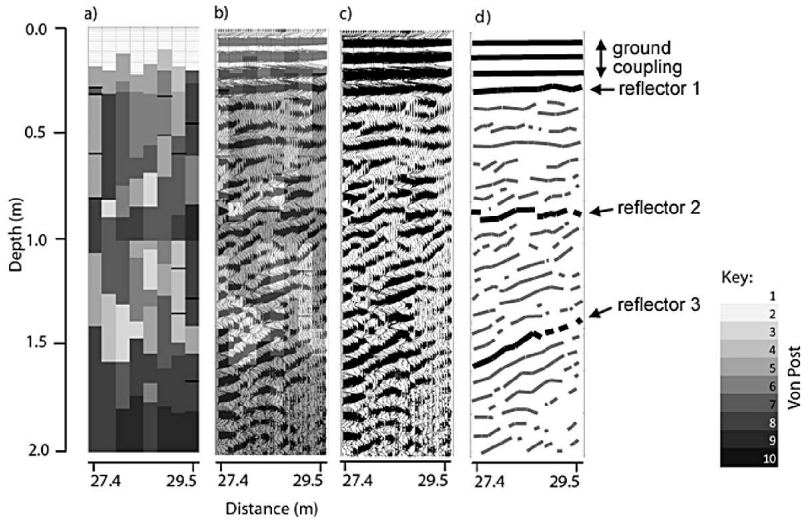

Figure 3. Comparison of high-resolution von Post measurements with the 225 MHz GPR. (a) The von Post measurements obtained at 0.30-m intervals. Boundaries in peat type that are not characterized by a shift in the von Post score are marked by a horizontal black line. (b) The 225 MHz common offset measurements obtained over the length of the high-resolution core data. Figures 3a and 3c are superimposed on Figure 3b for purposes of clarity. (d) Illustration of the key reflectors and ground coupling in the common offset measurements that are discussed within the text.

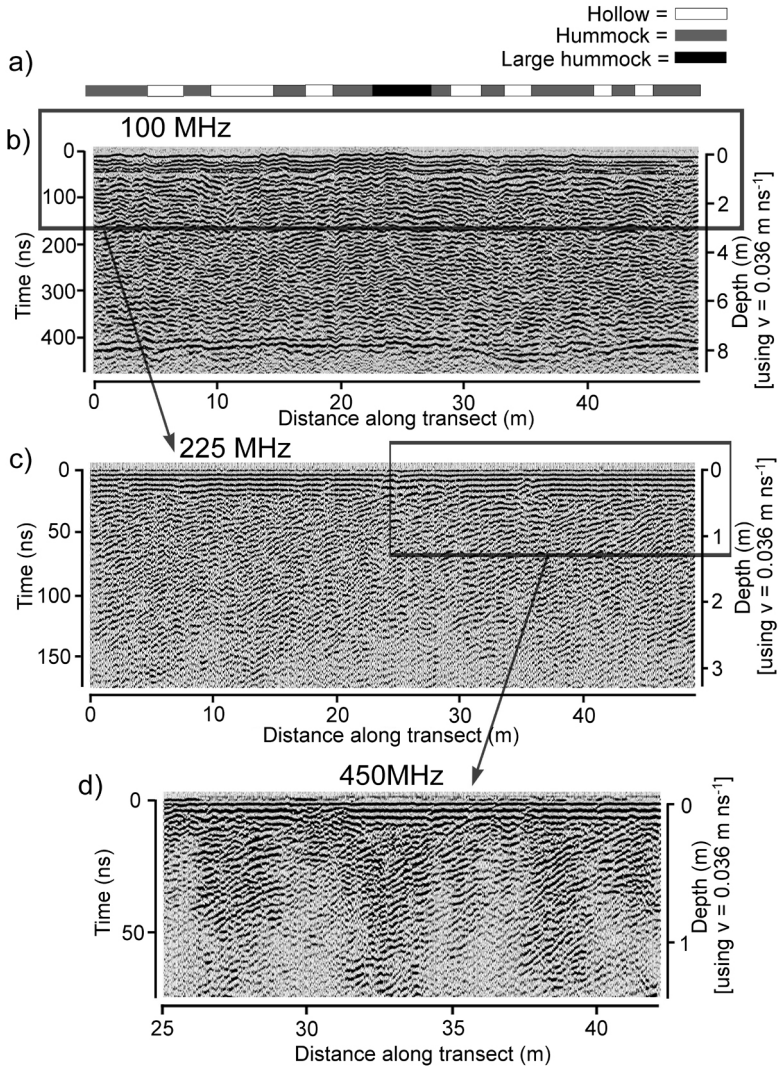

Figure 4. (a) Schematic of surface microforms along the length of the 45-m transect. Common offset measurements at a nominal frequency of (b)100 MHz, (c) 225 MHz and (d) 450 MHz. Note difference in depth scale between frequencies. Apparent horizontal boundary at approximate depths of 0–0.75 m, 0–0.25 m and 0–0.10 m results from ground coupling. See text and Figure 5 for details.

undulating, subparallel, and moderately continuous reflectors through the entire peat profile (Figure 4b). The pattern of reflectors at a frequency of 200 MHz did not vary substantially from that identified at a frequency of 100 MHz (data not shown). In comparison, common offset measurements at a frequency of 225 MHz showed a very different pattern of reflectors than those measured at 100 and 200 MHz (Figure 4c; note the different vertical scale). At 225 MHz, below the zone of ground coupling (depth 0–0.25 m) the reflectors showed a dipping structure through the transect, dipping in a northerly direction from the bottom left of the transect to the top right as represented in Figure 4c. The dip in the reflectors was most clearly identifiable at a depth of 0.8–2.0 m. Above this zone, at a depth of 0.3–0.8 m, the reflectors were more horizontal in nature. This dipping structure cannot be explained by small variations in surface topography along the transect. Common offsets measurements at a frequency of 450 MHz showed a similar pattern of diagonal reflectors (Figure 4d). However, penetration depths at this higher frequency were reduced to between 0.5 and 0.7 m within the drier hummock microforms and to approximately 1.25 m within the wetter hollow microforms where there was better coupling between the antenna and the peat. At 900 MHz the penetration depth was reduced to only 0.7 m within the wetter hollows (e.g., 2.5–5.0 m along the transect; Figure 5) and few reflectors were identifiable within the drier hummock microforms (e.g., 1–2 m). The 900 MHz measurements showed a predominately horizontal pattern of discontinuous reflectors, with a small section of discontinuous reflections at a distance of 3–4 m along the transect. This pattern corresponded with the more horizontal reflectors identified within the 225 MHz measurements between depths of 0.3 and 0.8 m.

3.3. Analysis of the Pattern of Reflections

[16] The determination of the apparent dip from the geometric attributes program confirmed the qualitative interpretation of the common offset measurements (Figure 6a).

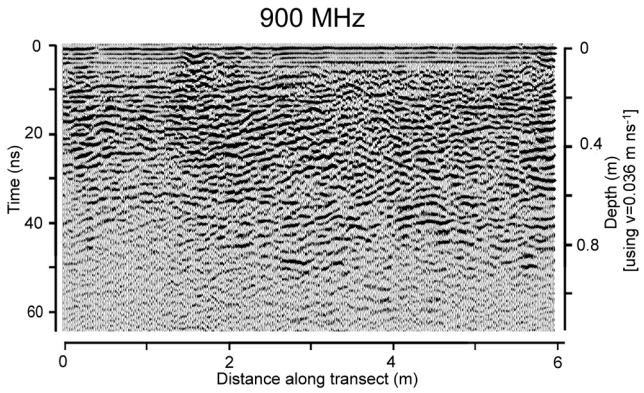

Figure 5. Common offset measurements at a nominal frequency of 900 MHz.

Northerly dips, characterized in red, dominated the reflection record along the length of the transect, with only 22% of the cross-sectional area characterized by southerly (blue) dips. Although the quantitative analysis highlights a strong uniformity in the angle of these reflectors, subtle spatial variations in the angle of the dip were identifiable both with depth and along the transect. The average dip angle with depth is presented in Figure 6b. The average angle remained relatively constant through the profile, between 0.8 and 2.5 m, averaging −3.9° (ranging between −4.5° and −3.5°; negative sign denotes northerly dip, positive sign denotes southerly dip). However, as suggested by the qualitative interpretation, the reflections became flatter above a depth of 0.8 m (the average angle of apparent dips equals approximately −1.75° at a depth of 0.5 m). Along the length of the transect (Figure 6c), the average dip cycles between −8° and 2° at a depth of 0.8–2.0 m. The cause of this cyclic behavior was unclear and cannot be explained by the slight topographic variation in the peat surface along the transect.

4. Analysis and Discussion

4.1. GPR Resolution

[17] The difference in the pattern of reflections between the low-frequency (≤200 MHz; e.g., Figure 4b) and the high-frequency (≥225 MHz; e.g., Figure 4c) antenna results from a significant increase in the central frequency within the Sensors and Software pulse EKKO systems. The 100 MHz antennas have a central frequency of 110 MHz. In comparison, the central frequency of the 225 MHz antennas is 240 MHz. The theoretical vertical resolution of common offset measurements is equal to one quarter of the EM wavelength [*Jol and Bristow*, 2003]. Assuming an EM velocity of 0.036 m s^{-1}, this equates to a resolution of 0.08 and 0.04 m for a central frequency of 110 and 240 MHz, respectively. However, such theoretical resolutions assume a return from a single reflector at a fixed distance [*Koppenjan*, 2009], whereas peatlands are characterized by multiple layers producing multiple returns. Range resolution, R_{res} (m), is the ability of GPR to resolve between such closely spaced targets, [*Koppenjan*, 2009]:

$$R_{res} = \frac{1.39c}{2f\varepsilon^{0.5}} \quad (1)$$

where c is the speed of light (m s^{-1}), f is the frequency (Hz) and ε is the dielectric permittivity (−). Central frequencies of 100, 130, 240, 370 and 980 MHz equate to range resolutions of 0.25, 0.19, 0.10, 0.07, 0.025 m, respectively.

[18] The cumulative distribution of peat layer thickness visually observed within both the 6.5-m and 2-m peat cores (Figure 2 and Figure 3a) is compared to the range resolutions calculated for the different GPR frequencies (Figure 7). The peat layers are on average 0.19 m thick. At nominal

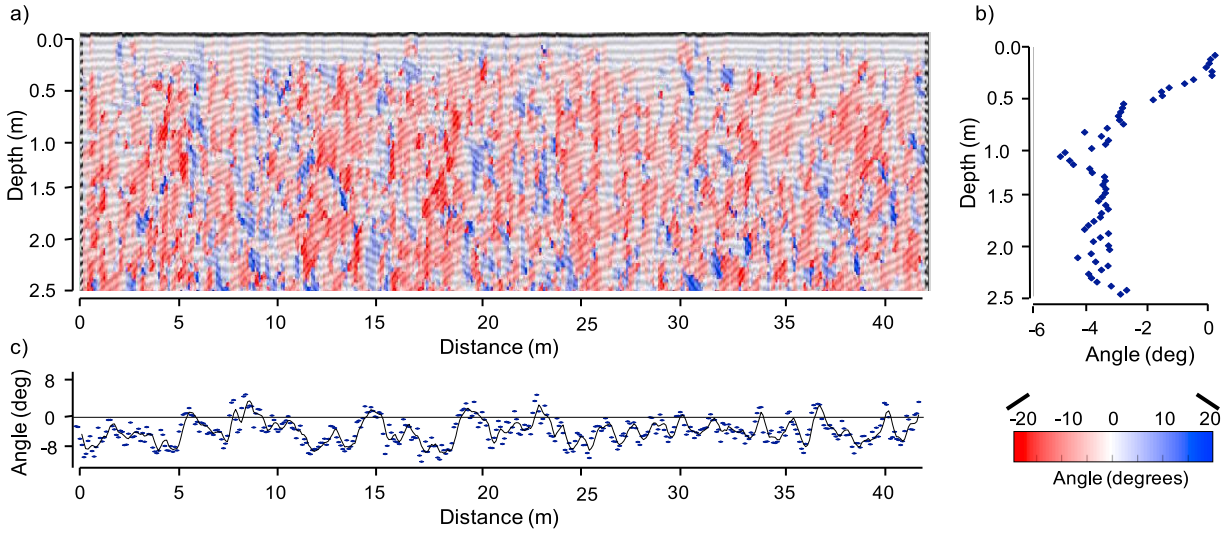

Figure 6. (a) Angle of dip within the 225 MHz common offset measurements. The angles of the dips, ranging from −20° to 20°, are represented by the color scale superimposed over the common offset measurements. (b) The average angle of the dips with depth through the peat profile at 0.04-m intervals, and (c) the average dip angle between a depth of 1.0 and 2.5 m with distance along the transect. The average calculated angle at 0.1-m intervals is represented by a blue symbol. The black line represents a running mean with $n = 4$.

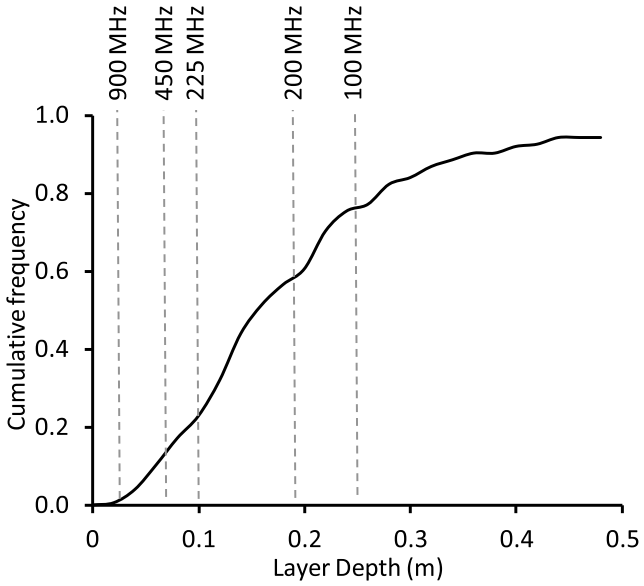

Figure 7. Cumulative frequency of peat layer thickness from all cores obtained along the transect. Marked for comparison are the range resolutions of the GPR measurements at nominal frequencies of 100, 200, 225, 450 and 900 MHz.

frequencies of 100 and 200 MHz, 75.4% and 57.5% of the visually observed peat layers are smaller than the range resolution, respectively. In comparison, at a nominal frequency of 225 MHz and 450 MHz, only 18% and 10%, respectively, of the visually observed peat layers are smaller than the range resolution. At lower frequencies (≤200 MHz) reflections are integrated across a number of layers. They provide only a very abstract representation of the subsurface peat structures and can only be applied to identify very distinct boundaries within Cors Fochno, notably the peat-mineral interface. Higher frequency common offset measurements are required to obtain a representative depiction of the pattern of subsurface reflectors. The 225 MHz antennas, with a 240 MHz central frequency, provide the best compromise between measurement resolution and penetration depth and are the focus of the subsequent discussion.

4.2. High-Resolution Peat Survey

[19] The boundaries identified within the high-resolution von Post measurements correspond to the pattern of reflections within the 225 MHz survey (Figures 3b–3d). The horizontal boundary at a depth of 0.3 m across all eight cores corresponds with a horizontal reflector in the common offset measurements (reflector 1 in Figure 3d). At a depth of 0.9–1.0 m, the zone of increased decomposition corresponds with a horizontal reflector across the radargram (reflector 2 in Figure 3d), and the transition to well-decomposed peat at a depth of 1.7 m coincides with a northerly dipping reflector (reflector 3 in Figure 3d), although the dip of this reflector is not clearly identifiable within the high spatial resolution von Post measurements. Reflections are also evident through the radargram that do not correspond clearly to boundaries within the high-resolution von Post survey. This lack of match highlights the difficulty in applying GPR to identify exact physical location of boundaries within the peat as demonstrated by *Worsfold et al.* [1986]. Problems in matching field data with radar reflections may result from a number of factors, including:

[20] 1. The Sensors and Software pulse EKKO supplies an EM wave pulse composed of a minimum of 1.5 wavelengths. Each individual reflector through the peat profile, therefore, produces more than one positive EM reflection identifiable within the radargram [cf. *Annan*, 2001].

[21] 2. The GPR system receives reflections from a 2-D footprint. Assuming an EM velocity of 0.036 m ns^{-1}, an antenna frequency of 240 MHz and an antenna separation of 0.5 m, the length of the footprint parallel to the transect, and its width perpendicular to the transect, are equal to 0.31 and 0.15 m at a depth of 1.0 m, respectively [*Annan*, 2001]. GPR provides an integrated measure of the reflections from this entire footprint.

[22] 3. The coring was performed at 0.3-m intervals and variations in peat physical properties will occur between these boundaries.

[23] 4. Although the von Post score will show some correlations with the dielectric permittivity of the peat, variations in the dielectric permittivity will also be associated with changes in peat saturation, porosity, and organic matter content that do not necessarily correspond with changes in the von Post classification and are not obvious to the naked eye. Bulk density, although more labor intensive to measure, would likely provide a more direct correlation with dielectric permittivity. While a close relationship between bulk density and humification has been identified by some authors [e.g., *Boelter*, 1969], other studies have indicated no significant correspondence [e.g., *Chason and Siegel*, 1986].

[24] Despite these limitations, it is evident that some of the more distinct reflectors do correspond to von Post changes in the peat properties (Figure 3).

4.3. Peatland Development History

[25] Although we have observed dipping features in just one transect within one peatland, they are distinct and raise questions concerning their formation and their significance for understanding peatland development. Horizontal reflectors within a peatland GPR image indicate bands of horizontal layers of different peat physical properties. Such transitions in peat physical properties result from the simultaneous change in the surface vegetation, near-surface hydrology or biogeochemical conditions across an area of peatland during its development. In comparison, a dipping boundary between the peat physical properties (dipping reflectors) suggest that such a transition did not occur simultaneously, but instead progressed across the peatland over time. To demonstrate this idea, we present a conceptual model of the development of a patterned peatland. Within the conceptual model, the peatland is composed of two different microforms (hummocks and hollows; Figure 8). At each time step (t), each microform lays down peat with its (the microform type's) characteristic physical properties (i.e., there is either hollow peat or hummock peat). In the first example (Figure 8a, at $t = 1$, the peatland is shallow and dominated by hollows. Over time ($t = 2$), hummocks spread across the peatland. This systematic change in microform type produces a single diagonal boundary between the two peat types (Figure 8a, $t = 5$). The GPR image (Figure 4c) highlights multiple dipping reflections through the profile, suggesting

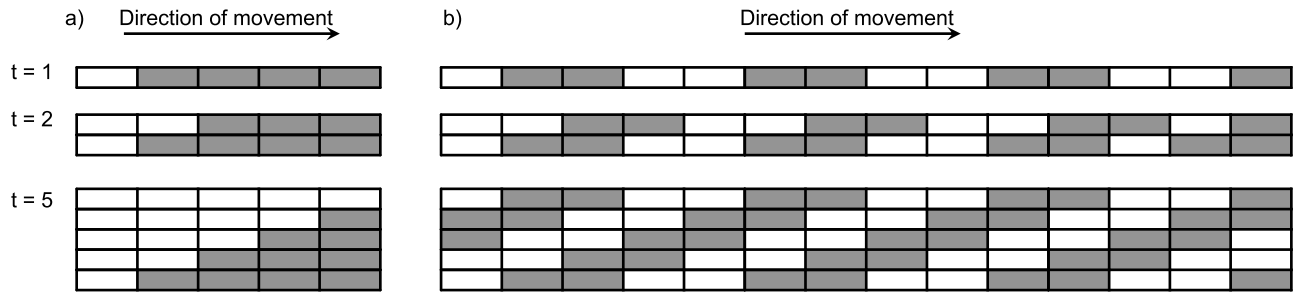

Figure 8. Conceptual model representing the formation of (a) a single and (b) multiple dipping reflectors through a peat profile. The cross sections of two peatlands are shown over time (t; from t = 1–5). Gray boxes represent peat formed under hollows, white boxes represent peat formed under hummocks. A single box of peat is laid down during each time step (t). In Figure 8a the peat surface is initially dominated by hollow microforms, and over the course of the five time steps (t = 1 to t = 5), the hummock microforms migrate across the peat surface from left to right. In Figure 8b the peat surface is initially dominated by bands of hummocks and hollows across the peat surface, which all migrate from left to right over the five time steps.

the movement of multiple microforms across the peat surface through time. The second example (Figure 8b) is therefore initially composed of a repeating pattern of hummocks and hollows. These microforms migrate steadily across the peatland over time. By t = 5, this produces multiple diagonal columns of peat, with diagonal interfaces similar to those observed within the high frequency GPR measurements. The northerly dip in the GPR reflections indicate that the surface microforms are moving in a southerly direction (from left to right within Figure 4) and thus are moving downslope as the peatland grows.

[26] The formation of diagonal columns of peat would account for the measured fluctuations through the peat profile between *Sphagnum* rich and sedge rich peat and peat of different structures (section 3.1). Vertical peat cores would intersect the diagonal columns, thus sampling alternating peat types. Assuming an average dip of −3.9 degrees and an average microform width of 2.8 m (Figure 4a), such diagonal columns would produce vertical layers 0.19 m in thickness through the core. The thickness of these vertical layers is equal to the average peat layer thickness obtained from coring (0.19 m; section 4.1). From analysis of the peat cores alone, it is unclear whether any of the transitions between peat types occur at the same depth (at the same time) within multiple cores (such as is observed by *Ellis and Tallis* [2000]) suggesting a widespread transition in the surface vegetation, or whether the observed transitions occur independently between the different core locations, suggesting a horizontal migration of the microforms (radiometric dating or regional pollen statigraphy would be required to confirm which of these two alternatives was the case). Small sections of the peat cores do vary in unison. For example, within the top 0.5 m of all three cores there is a low abundance of sedges to *Sphagnum* at the surface, a high abundance at a depth of 0.25 m and a low abundance of sedge remains at a depth of 0.5 m (Figure 2b). Beyond this near-surface zone, any correspondence between the different cores is difficult to identify. Further peat cores would be required to evaluate any such correlations in detail [see, for example, *Barber et al.*, 1998].

[27] In addition to the movement through time of peat microforms, the observed pattern of diagonal reflectors could indicate different developmental pathways. We outline briefly how such pathways, including differential subsidence, past peat slopes and slumping could produce the observed pattern of diagonal reflectors and explain why such development pathways are unlikely.

[28] *Differential subsidence*: Recent (within the last 1000 years) differences in the rate of subsidence along the length of the transect could cause peat profiles that had formed horizontally over the development of the peatland to collapse producing a pattern of diagonal reflectors. However, considering there appears to be a relatively homogenous pattern of diagonal reflectors along the length of the transect

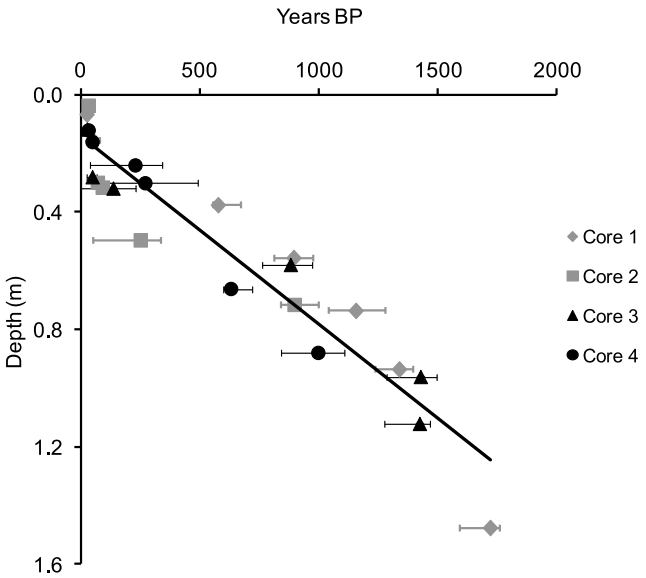

Figure 9. Relationship between peat age and depth for four cores across Cors Fochno taken and analyzed by *Schulz* [2004] (based on original figures by *Schulz* [2004]). Measurements were obtained using a combination of radiocarbon dating and spheroidal carbonaceous particle analysis.

between a depth of 0.5 and 2.5 m, the formation of such dipping reflectors would require an unrealistic 2.0-m collapse of the lower 4.0-m deep peat at one end of the transect while the other end remained fixed.

[29] *Past peat slopes*: The peatland may have originally consisted of multiple domes where the areas between the domes became infilled to produce a single peatland. If that was the case, diagonal slopes directed to the interior of the current peatland may be observed. The formation of the measured 3.9° slopes would require an elliptical peatland dome with a diameter of 120 m and a highest point of the dome of 6 m above the peatland margin. An unrealistic number of such peatlands would have been required to form the current single peat dome and there is no evidence for such development in the paleo record of Cors Fochno [*Schulz*, 2004].

[30] *Slumping*: Slumping of the peat surface could explain the formation of diagonal layers within the peat profile. However, this would indicate the downslope movement of material directed toward the center of the peatland dome, which is clearly impossible.

[31] While a more comprehensive geophysical and paleoecological survey is required to determine the evolution of this patterned peatland, the movement of peatland surface microforms over time appears to provide the most plausible explanation of our data.

[32] *Schulz* [2004] combined radiocarbon dating and spheroidal carbonaceous particle analysis to derive age-depth relationships for four cores obtained from both the marginal and central regions of Cors Fochno. While fine scale complexities are identifiable in the age-depth relationship within each core [*Schulz*, 2004], there is a general linear relationship between peat age and depth through the top 1.5 m of the peat profile (that measured by *Schulz* [2004]) across all cores (Figure 9; $R^2 = 0.90$). This linear relationship indicates an average growth rate over this top 1.5 m of 0.063 m per 100 years. Assuming dip angles between the different peat types of −3.9°, equal to the average angle of the dipping reflectors (section 4.3), the horizontal movement through time of the surface vegetation cover is equal to 9.8 mm per year. Such small variation in this surface vegetation cover would be very difficult to verify from physical observations, with less than 0.1 m of movement per decade (with less movement within the last 1200 years; top 0.8 m).

[33] The movement of microforms suggested by our data is similar to the simulated downslope movement of hummocks and hollows in the models of *Swanson and Grigal* [1988] and *Couwenberg and Joosten* [2005], but a range of different factors and processes may be involved in peatland pattern formation [*Eppinga et al.*, 2009]. Further research is required on a range of transects within different peatlands to provide insight on the ecohydrological controls on pattern formation and to link transect information with mathematical models that simulate peatland patterning and changes in pattern over time [cf. *Morris et al.*, 2011; *Baird et al.*, 2012].

5. Conclusions

[34] GPR has been used to characterize the statigraphy of a patterned peatland and to infer its developmental history. We have shown that an important compromise between survey depth and resolution is necessary in the design of a peatland GPR stratigraphical survey. The thinness of many peat layers (at least within the site studied here) means that high frequency measurements (central frequency equal to 240 MHz) with a lower penetration depth must be applied to characterize adequately the subsurface structures of the peatland. As a result, the detailed peat stratigraphy is identifiable only to a depth of approximately 2.5 m using widely available GPR equipment. Even with such a high frequency approach, transitions in peat physical properties are only identifiable if the layers are ≥0.10 m thick; i.e., the period between transition in peat plant communities or hydrological conditions is greather than 160 years (assuming a peat growth rate of 0.63 m per 1000 years). In addition, while we have focused here on determining the vertical resolution limits of GPR surveys, the horizontal resolution may also restrict its application. Although the calculated horizontal footprint of the GPR survey (0.31 m × 0.15 m) is below that of the surface microforms, the variation in peat profiles within this footprint and its impact on the GPR survey remain uncertain.

[35] The high frequency GPR measurements have shown a striking pattern of subsurface reflections that are dipping consistently in a northern direction across the peat profile. Further research is required to map the angle and direction of the dipping reflectors across different regions of this and other peatlands, specifically within the central dome and rand. Determining the extent to which the dipping reflections vary with slope, hydraulic conductivity [*Baird et al.*, 2008] or between regions with different relative proportions of hummocks and hollows [*Belyea*, 2007] could provide important information about ecohydrological controls on peatland pattern formation and wider peatland development.

[36] **Acknowledgments.** The authors are grateful to the Editor, Associate Editor and two anonymous reviewers for comments on an earlier version of this manuscript. We are also grateful to Joseph Doetsch for use of the geometric attributes program and to the Countryside Council for Wales for kindly providing access to the field site. The authors would also like to thank Nikki Dodd (University of Leeds) for the kite-borne aerial photograph, the Natural Environment Research Council Airborne Survey and Research Facility (ARSF) for collection of LiDAR data (GB08/12) and Henry Lamb (University of Aberystwyth) for the loan of one of the Russian corers. Financial support was provided by the UK Natural Environment Research Council (grant NE/F004958/1) and by a Natural Sciences and Engineering Research Council (NSERC) of Canada Discovery Supplement to JMW.

References

Annan, A. P. (2001), *Ground Penetrating Radar Workshop Notes*, 197 pp., Sensors and Software, Mississauga, Ontario, Canada.

Baird, A. J., P. A. Eades, and B. W. J. Surridge (2008), The hydraulic structure of a raised bog and its implications for ecohydrological modelling of bog development, *Ecohydrology*, *1*, 289–298, doi:10.1002/eco.33.

Baird, A. J., L. R. Belyea, and P. Morris (2009), Upscaling peatland-atmosphere fluxes of carbon gases: Small-scale heterogeneity in process rates and the pitfalls of "bucket-and-slab" models, in *Carbon Cycling in Northern Peatlands*, *Geophys. Monogr. Ser.*, vol. 184, edited by A. J. Baird et al., pp. 37–53, AGU, Washington, D. C., doi:10.1029/2008GM000826.

Baird, A. J., P. Morris, and L. R. Belyea (2012), The DigiBog peatland development model 1: Rationale, conceptual model, and hydrological basis, *Ecohydrology*, *5*, 242–255, doi:10.1002/eco.230.

Barber, K. (1981), *Peat Stratigraphy and Climate Change: A Palaeoecological Test of the Theory of Cyclic Peat Bog Regeneration*, A.A. Balkema, Rotterdam, Netherlands.

Barber, K., L. Dumayne-Peaty, P. Hughes, D. Mauquoy, and R. Scaufe (1998), Replicability and variability of the recent macrofossil and proxy-climate record from raised bogs: Field stratigraphy and macrofossil data

from Bolton Fell Moss and Walton Moss, Cumbria, England, *J. Quat. Sci.*, *13*, 515–528, doi:10.1002/(SICI)1099-1417(1998110)13:6<515::AID-JQS393>3.0.CO;2-S.

Belyea, L. R. (2007), Climatic and topographic constraints on the abundance of bog pools, *Hydrol. Processes*, *21*, 675–687, doi:10.1002/hyp.6275.

Belyea, L. R. (2009), Nonlinear dynamics of peatlands and potential feedbacks on the climate system. Carbon Cycling in Northern Peatlands, in *Carbon Cycling in Northern Peatlands*, *Geophys. Monogr. Ser.*, vol. 184, edited by A. J. Baird et al., pp. 5–18, AGU, Washington, D. C., doi:10.1029/2008GM000829.

Belyea, L. R., and N. Malmer (2004), Carbon sequestration in peatland: Patterns and mechanisms of response to climate change, *Global Change Biol.*, *10*, 1043–1052, doi:10.1111/j.1529-8817.2003.00783.x.

Boatman, D. J., and R. W. Tomlinson (1973), The Silver Flowe I. Some structural and hydrological features of British bog and their bearing on pool formation, *J. Ecol.*, *61*, 653–666, doi:10.2307/2258641.

Boelter, D. H. (1969), Physical properties of peats as related to degree of decomposition, *Soil Sci. Soc. Am. Proc.*, *33*, 606–609, doi:10.2136/sssaj1969.03615995003300040033x.

Bubier, J., A. Costello, T. R. Moore, N. T. Roulet, and K. Savage (1993), Microtopography and methane flux in boreal peatlands, northern Ontario, Canada, *Can. J. Bot.*, *71*, 1056–1063, doi:10.1139/b93-122.

Chason, D., and D. Siegel (1986), Hydraulic conductivity and related physical properties of peat, Lost River Peatland, northern Minnesota, *Soil Sci.*, *142*, 91–99, doi:10.1097/00010694-198608000-00005.

Comas, X., and L. Slater (2009), Noninvasive field-scale characterization of gaseous-phase methane dynamics in peatlands using the ground-penetrating radar method, in *Carbon Cycling in Northern Peatlands*, *Geophys. Monogr. Ser.*, vol. 184, edited by A. J. Baird et al., pp. 159–171, AGU, Washington, D. C., doi:10.1029/2008GM000810.

Comas, X., L. Slater, and A. Reeve (2004), Geophysical evidence for peat basin morphology and stratigraphic controls on vegetation observed in a Northern Peatland, *J. Hydrol.*, *295*, 173–184, doi:10.1016/j.jhydrol.2004.03.008.

Couwenberg, J., and H. Joosten (2005), Self-organization in raised bog patterning: The origin of microtope zonation and mesotope diversity, *J. Ecol.*, *93*, 1238–1248, doi:10.1111/j.1365-2745.2005.01035.x.

Ekono, Inc. (1981), Report on energy use of peat, paper presented at the U.N Conference on New and Renewable Sources of Energy, Nairobi, Kenya, 10–21 August.

Ellis, C. J., and J. H. Tallis (2000), Climatic control of blanket mire development at Kentra Moss, north-west Scotland, *J. Ecol.*, *88*, 869–889, doi:10.1046/j.1365-2745.2000.00495.x.

Eppinga, M. B., P. C. de Ruiter, M. J. Wassen, and M. Rietkerk (2009), Nutrients and hydrology indicate the driving mechanisms of peatland surface patterning, *Am. Nat.*, *173*, 803–818, doi:10.1086/598487.

Foster, D. R., and S. C. Fritz (1987), Mire development, pool formation and landscape processes on patterned Fens in Dalarna, central Sweden, *J. Ecol.*, *75*, 409–437, doi:10.2307/2260426.

Gorham, E. (1991), Northern peatlands–role in the carbon cycle and probable responses to climatic warming, *Ecol. Appl.*, *1*, 182–195, doi:10.2307/1941811.

Jol, H. M., and C. S. Bristow (2003), GPR in sediments: Advice on data collection, basic processing and interpretation, a good practice guide, *Geol. Soc. Spec. Publ.*, *211*, 9–27, doi:10.1144/GSL.SP.2001.211.01.02.

Jol, H. M., and D. G. Smith (1995), Ground penetrating radar surveys of peatlands for oilfield pipelines in Canada, *J. Appl. Geophys.*, *34*, 109–123, doi:10.1016/0926-9851(95)00018-6.

Kettridge, N. and Baird, A. J. (2010) Simulating the thermal behavior of northern peatlands with a 3-D microtopography, *J. Geophys. Res.*, *115*, G03009, doi:10.1029/2009JG001068.

Koppenjan, S. (2009), Ground penetrating radar systems and design, in *Ground Penetrating Radar – Theory and Applications*, edited by H. M. Jol, pp. 73–97, Elsevier, Amsterdam, doi:10.1016/B978-0-444-53348-7.00003-X.

Marfurt, K. J., R. L. Kirlin, S. L. Framer, and M. S. Bahorich (1998), 3-D seismic attributes using a semblance-based coherency algorithm, *Geophysics*, *63*, 1150–1165.

McClymont, A. F., A. G. Green, R. Streich, H. Horstmeyer, J. Tronicke, D. C. Nobes, J. Pettinga, J. Campbell, and R. Langridge (2008), Visualization of active faults using geometric attributes of 3D GPR data: An example from the Alpine Fault Zone, New Zealand, *Geophysics*, *73*(2), B11–B23.

Morris, P., L. R. Belyea, and A. J. Baird (2011), Ecohydrological feedbacks in peatland development: A theoretical modelling study, *J. Ecol.*, *99*, 1190–1201, doi:10.1111/j.1365-2745.2011.01842.x.

Neal, A. (2004), Ground-penetrating radar and its use in sedimentology: Principles, problems and progress, *Earth Sci. Rev.*, *66*, 261–330, doi:10.1016/j.earscirev.2004.01.004.

Reynolds, J. M. (1994), *An Introduction to Applied and Environmental Geophysics*, Wiley and Sons, New York.

Schulz, J. (2004), Palaeoecological approach using high-resolution macrofossil analysis, PhD thesis, Fac. of Eng., Sci. and Math., Univ. of Southampton, Southampton, UK.

Slater, L. D., and A. S. Reeve (2002), Investigating peatland stratigraphy and hydrogeology using integrated electrical geophysics, *Geophysics*, *67*, 365–378.

Swanson, D. K., and D. F. Grigal (1988), A simulation model of mire patterning, *Oikos*, *53*, 309–314, doi:10.2307/3565529.

Tallis, J. H. (1994), Pool-and-hummock patterning in a southern pennine blanket Mire II. The formation and erosion of the pool system, *J. Ecol.*, *82*, 789–803, doi:10.2307/2261444.

Theimer, B. D., D. C. Nobes, and B. G. Warner (1994), A study of the geoelectrical properties of peatlands and their influence on ground-penetrating radar surveying, *Geophys. Prospect.*, *42*, 179–209, doi:10.1111/j.1365-2478.1994.tb00205.x.

Turunen, J., E. Tomppo, K. Tolonen, and A. Reinikainen (2002), Estimating carbon accumulation rates of undrained mires in Finland – Application to boreal and subarctic regions, *Holocene*, *12*, 69–80, doi:10.1191/0959683602hl522rp.

Ulriksen, C. P. F. (1980), Investigation of peat thickness with radar, in *Proceedings of the Sixth International Peat Congress, Duluth, Minnesota, 1980*, pp. 126–129, Int. Peat Soc., Jyväskylä, Finland.

von Post, L., and E. Granlund (1926), Sodra Sveriges Tortillangar I, *Sver. Geol. Unders., Årsb. 19, Ser. C.*, *335*, 127 pp.

Waddington, J. M., and N. T. Roulet (1996), Atmosphere-wetland carbon exchanges: Scale dependency of CO_2 and CH_4 exchange on the developmental topography of a peatland, *Global Biogeochem. Cycles*, *10*, 233–245, doi:10.1029/95GB03871.

Walker, D., and P. M. Walker (1961), Stratigraphic evidence of regeneration in some Irish bogs, *J. Ecol.*, *49*, 169–185, doi:10.2307/2257432.

Warner, B. G., D. C. Nobes, and B. D. Theimer (1990), An application of ground penetrating radar to peat stratigraphy of Ellice Swamp, southwestern Ontario, *Can. J. Earth Sci.*, *27*, 932–938, doi:10.1139/e90-096.

Whittington, P. N., and J. S. Price (2006), The effects of water table drawdown (as a surrogate for climate change) on the hydrology of a fen peatland, Canada, *Hydrol. Processes*, *20*, 3589–3600, doi:10.1002/hyp.6376.

Worsfold, R. D., S. K. Parashar, and T. Perrot (1986), Depth profiling of peat deposits with impulse radar, *Can. Geotech. J.*, *23*, 142–154, doi:10.1139/t86-024.